

Reactions of periodontal ligament epithelial cell clusters and OX6-immunopositive cells to experimental tooth movement and periodontitis

O. Tadokoro¹, I. Kawahara²,
V. Vandevska-Radunovic³

¹Department of Oral Anatomy 1, School of Dentistry, Matsumoto Dental University, Nagano, Japan, ²Division of Hard Tissue Research, Matsumoto Dental University, Graduate School, Nagano, Japan and ³Department of Orthodontics, Institute of Clinical Dentistry, University of Oslo, Oslo, Norway

Tadokoro O, Kawahara I, Vandevska-Radunovic V. Reactions of periodontal ligament epithelial cell clusters and OX6-immunopositive cells to experimental tooth movement and periodontitis. J Periodont Res 2011; 46: 584–591. © 2011 John Wiley & Sons A/S

Background and Objective: The aim of this study was to investigate reactions of periodontal ligament epithelial cell clusters and major histocompatibility complex class II (OX6)-immunopositive cells to simultaneously induced tooth movement and periodontitis employing Waldo's method.

Material and Methods: Elastic gums were inserted between the right upper first and second molars of rats. Animals were killed by intracardiac perfusion on days 1, 3, 7 and 14 after the experimental procedures, and maxillary molars were decalcified and processed for OCT compound. Cytokeratin and OX6 antibodies to detect epithelial and immunocompetent cells were used for double-fluorescence immunohistochemistry. Immunostained sections of rat upper molar regions were examined with a fluorescence microscope.

Results: Large periodontal ligament epithelial cell clusters appeared and became contiguous with each other, and OX6-immunopositive cells surrounded the clusters over time in the periodontal ligament near the gum insertion site. In the periodontal ligament distant from the gum insertion site, epithelial cell clusters and OX6-immunopositive cells were scattered. After 14 d, thickened epithelium and elongated rete pegs were found close to large epithelial cell clusters in the periodontal ligament near the gum insertion site.

Conclusion: These findings suggest proliferation and/or aggregation of periodontal ligament epithelial cells, and interaction between OX6-immunopositive cells and the periodontal ligament epithelial cells, in response to tooth movement and periodontal inflammation. This method may be a useful experimental model to elucidate the relationship between rete pegs and periodontal ligament epithelial cell clusters in inflammatory conditions.

Dr Osamu Tadokoro, Department of Oral Anatomy 1, School of Dentistry, Matsumoto Dental University, Nagano, Japan
Tel: +81 263 51 2034
Fax: +81 263 53 3456
e-mail: osamut@mdu.ac.jp

Key words: CK immunopositive cells; epithelial cell rests of malassez; inflammation; in vivo model; OX6 immunopositive cells; periodontal ligament

Accepted for publication March 29, 2011

Periodontal ligament epithelial cell clusters, which are known as epithelial cell rests of Malassez, are distributed around the tooth root as a mesh-like structure. These cell clusters can be observed as oval or round shapes, close to the tooth root surface (1,2). In rat periodontal tissue, epithelial cell clusters are distributed not only near the root surface but also proximal to blood vessels, between root dentin and cementum, and in the surface concavity and inside the alveolar bone (3). The main skeletal protein of the epithelial cells cytoplasm is the keratin filament (cytokeratin, CK), a feature that has been used to demonstrate and differentiate the periodontal epithelial cells from periodontal fibroblasts and cementoblasts (3–5).

The periodontal Malassez cell rests are differentiated cells, mostly arrested in interphase, but it has been clearly established that they are capable of re-entering the cell cycle and proliferating in certain conditions. For example, morphological changes, ³H-thymidine uptake and a positive bromo-deoxyuridine reaction in epithelial cell clusters have been shown to occur during experimental tooth movement (6,7). The epithelial proliferation is apparently associated with inflammation and local accumulation of various types of immune cells (8).

Both epithelial cell clusters and immunocompetent cells [major histocompatibility complex class II (OX6)-immunopositive and ED1-immunopositive cells] are present in the region near the oral cavity and in the root furcation area (3,9). Immunohistochemical and immunoelectron microscopic observations confirm that nonepithelial, immunocompetent cells are in close contact with epithelial cell rests of Malassez in noninflamed rat periodontal tissue (3,10). Characteristics of these cells indicate their possible interaction and involvement in the biological defense system of the periodontal ligament (3); however, there are no functional experimental studies confirming this possibility.

Experimental tooth movement is brought about by inflammatory tissue changes that involve, among other factors, immunocompetent cells (11).

Knowing that it also affects the morphology of epithelial cell rests of Malassez (7,12,13), experimental tooth movement seems to be a suitable model for the investigation of a joint response of the periodontal epithelial and OX6-immunopositive cells in an inflammatory setting. For this purpose, an elastic gum was inserted between the first and second upper molars of adult rats, inducing experimental tooth movement, as well as periodontitis. The reactions of the epithelial and OX6-immunopositive cells were investigated with a fluorescence microscope. The hypothesis is that experimental tooth movement leads to proliferation of epithelial and OX6-immunopositive cells in rat molars.

Material and methods

Animals and tissue preparation

This study was performed after approval by the Experimental Animal Ethics Committee of Matsumoto Dental University. In Wistar rats (7-wk-old males weighing about 170 g, three animals per day, 15 animals in total), elastic gum (about 0.5 mm thick) was carefully inserted between the upper right first and second molars following the method reported by Waldo *et al.* (Fig. 1). The animals were deeply anesthetized with sodium pentobarbital after 1,3,7, or 14d, and they were transcidentally perfused with 4% paraformaldehyde. After fixation, the upper jaw regions, including the molars, were excised and fixed in the same fixative overnight.

The sample was then decalcified in 5% EDTA for 21 d, embedded in OCT compound and frozen in liquid nitrogen. Serial sections (~6 µm thick) in a horizontal direction were prepared from the embedded samples, from the region near the junctional epithelium to the region above the alveolar bone, using a cryostat and mounted on aminopropyltriethoxysilane-coated slide glasses.

Immunohistochemistry

Immunohistochemical staining was performed as previously reported (3). After washing with phosphate-buffered

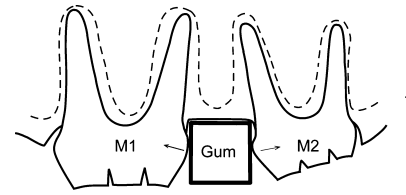


Fig. 1. The positional relationship between the rat upper molars and inserted elastic gum in the sagittal plane is shown. Gum was inserted in the interdental papilla between the first (M1) and second molars (M2).

saline several times, the slides were placed in normal goat serum for 30 min, followed by incubation with anti-CK antibody (Nihirei Biosciences, Tokyo, Japan) and 1000-fold dilution of anti-OX6 antibody (Serotec Co., Ltd, Oxford, UK) as the primary antibodies for 60 min at room temperature. After washing with phosphate-buffered saline several times, the sections were incubated with 100-fold dilutions of anti-rabbit IgG to anti-CK (Alexa Fluor 594; Invitrogen Corp. Carlsbad, CA, USA) and anti-mouse IgG to anti-OX6 (Alexa Fluor 488; Invitrogen Corp.) for 30 min. After washing with phosphate-buffered saline, aqueous mounting medium containing 4',6-diamidino-2-phenylindole dihydrochloride (DAPI; Invitrogen Corp.) was dripped onto the sections, and they were coverslipped. Specificity of the anti-CK and anti-OX6 antibodies was confirmed by replacing them with phosphate-buffered saline or normal goat serum. The stained sections were observed under a fluorescence microscope (Olympus BX-50; Olympus, Tokyo, Japan) and photographed using a digital image acquisition device (DP50; exposure time 1.5 s). Observation areas were divided into two regions: bucco-cervical (c) and furcational (f) regions, and the reactions of cells immunostaining positive for CK and OX6 in each region were observed (Fig. 2).

Statistical analysis

Five sample sections (at least three sections apart) in each region on each day were selected for the analysis. For the purpose of quantitative evaluation of the CK- and OX6-immunopositive cells, the area of the samples was examined using a 3CCD color video

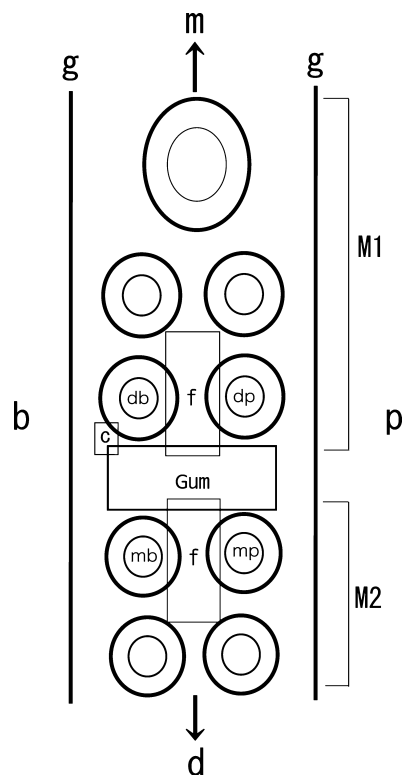


Fig. 2. The positions of the roots of the rat upper molars, inserted elastic gum, and observed regions (c, bucco-cervical region; f, furcational region) in the horizontal plane are shown. Abbreviations: b, buccal site; d, distal site; db, disto-buccal root; dp, disto-palatal root; g, gingiva; m, mesial site; mb, mesio-buccal root; mp, mesio-palatal root; M1, first molar; M2, second molar; p, palatal site.

camera (DP50; Olympus) mounted on a standard fluorescence microscope (BX50; Olympus). A drawing of the contour of the area was made on the screen of a multiscan color computer display (Apple Computer Inc., Cupertino, CA, USA) and then digitized with a two-dimensional analysis system (Mac SCOPE; Mitani Corp., Tokyo, Japan) connected to a Macintosh computer system (Power Mac G4; Apple Computer Inc.). The average rates (stained area/observed area \times 100) were calculated in each group. The average rate of CK- and OX6-immunopositive cells in the defined regions was counted, and means and standard deviations calculated for each experimental period. One-way ANOVA was used to evaluate the differences between the experimental periods for CK- and OX6-immunopositive cells in bucco-

cervical (c) and furcational (f) areas, respectively. The level of statistical significance was set at $p < 0.05$.

Results

The CK-immunopositive cells rate increased significantly after 3 d and remained significantly increased at 7 and 14 d (Fig. 3A,B) in both the buccal and the furcational area. The rate of OX6-immunopositive cells significantly increased at 3 d in the buccal periodontal ligament (Fig. 4A), but decreased at 1 and 3 d in the furcational area (Fig. 4B). No other significant changes were noticed.

Control

Cervical region— A CK-immunopositive reaction was noted in the gingival epithelium and cell clusters near the root surface (Fig. 5A). Immunopositive cell clusters consisting of about three to six cells were spindle or oval shaped and aligned along the root surface at fairly regular intervals (arrowheads in Fig. 5A). The distances of the cell clusters from the root surface were mostly equal. An OX6-positive reaction was observed in cells extending cytoplasmic processes along periodontal ligament fibers. The OX6-immunopositive cells were mainly distributed in connective tissue immediately below the gingival epithelium, near the root surface, and around CK-immunopositive cell clusters (Fig. 5A).

Furcational region— A CK-immunopositive reaction was noted in round or oval cell clusters larger than those in the cervical region (Fig. 5B). Many CK-immunopositive cell clusters were aligned at fairly regular intervals along the root surface (Fig. 5B), but were also often observed in regions distant from the root surface. The size and shape of the cell clusters were similar, but large cell clusters with an irregular morphology were occasionally observed. OX6-immunopositive reactions were noted in cells with diverse morphologies, such as cells with long, thin or thick, short cytoplasmic processes and round cells. As observed in the cervical region, OX6-immunopositive cells contiguous with

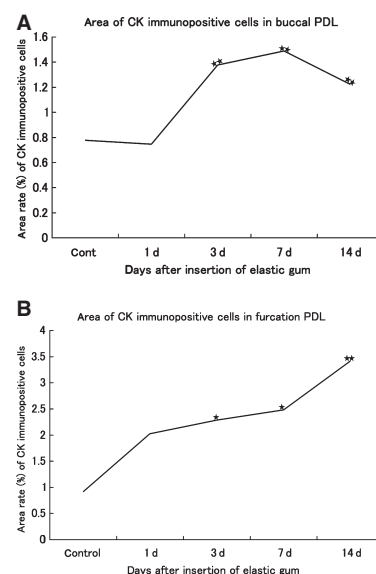


Fig. 3. The area rate of CK-immunopositive cells in the buccal (A) and furcational periodontal ligament (B) in the control specimens and at 1, 3, 7 and 14 d after the insertion of the elastic gum. * $p < 0.05$ and ** $p < 0.01$.

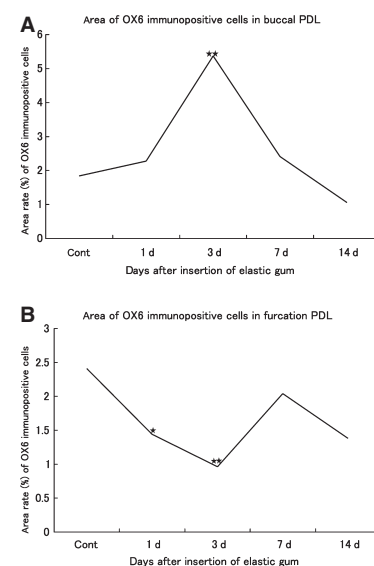


Fig. 4. The area rate of OX6-immunopositive cells in the buccal (A) and furcational periodontal ligament (B) in the control specimens and at 1, 3, 7 and 14 d after the insertion of the elastic gum. * $p < 0.05$ and ** $p < 0.01$.

CK-immunopositive cell clusters were present (Fig. 5B).

Periodontal ligament after 1 d

Cervical region— A CK-immunopositive reaction was observed in the

gingival epithelium and cell clusters near the root surface (Fig. 5C). Cell clusters in connective tissue near the gingival epithelium pressed by the gum were round or oval and aligned at fairly regular intervals along the root surface (Fig. 5C). The distances of the cell clusters from the root surface were mostly equal. An OX6-immunopositive reaction was observed in cells extending dendrites into connective tissue (Fig. 5C), but rarely noted near the root surface and around CK-immunopositive cell clusters.

Furcational region— A CK-immunopositive reaction was noted in round or oval cell clusters (Fig. 5D). The cell cluster distribution was similar to that in the control sections, but large cell clusters were often present (Fig. 5D), showing a difference in the cell cluster size. An OX6-immunopositive reaction was observed in cells with an irregular morphology, as seen in the control sections. The OX6-immunopositive cells were widely distributed generally and were also noted around CK-immunopositive cell clusters (Fig. 5D).

Periodontal ligament after 3 d

Cervical region— A CK-immunopositive reaction was noted in the gingival epithelium and oval or long oval cell clusters near the root surface (Figs 5E and 6). The distances of the cell clusters from the root surface were fairly equal. In connective tissue near the gingival epithelium pressed by the gum, large cell clusters were often present and the clusters were contiguous with each other (Fig. 5E). An OX6-immunopositive reaction was noted in cells with an irregular morphology and widely distributed in the periodontal ligament (Fig. 5E). In the periodontal ligament slightly distant from the gingival epithelium, OX6-immunopositive cells often extended cytoplasmic processes to the root surface and epithelial cell clusters (Fig. 6).

Furcational region— A CK-immunopositive reaction was noted in round or oval cell clusters (Fig. 5F). The cell cluster distribution was similar to that on day 1, but larger cell clusters were

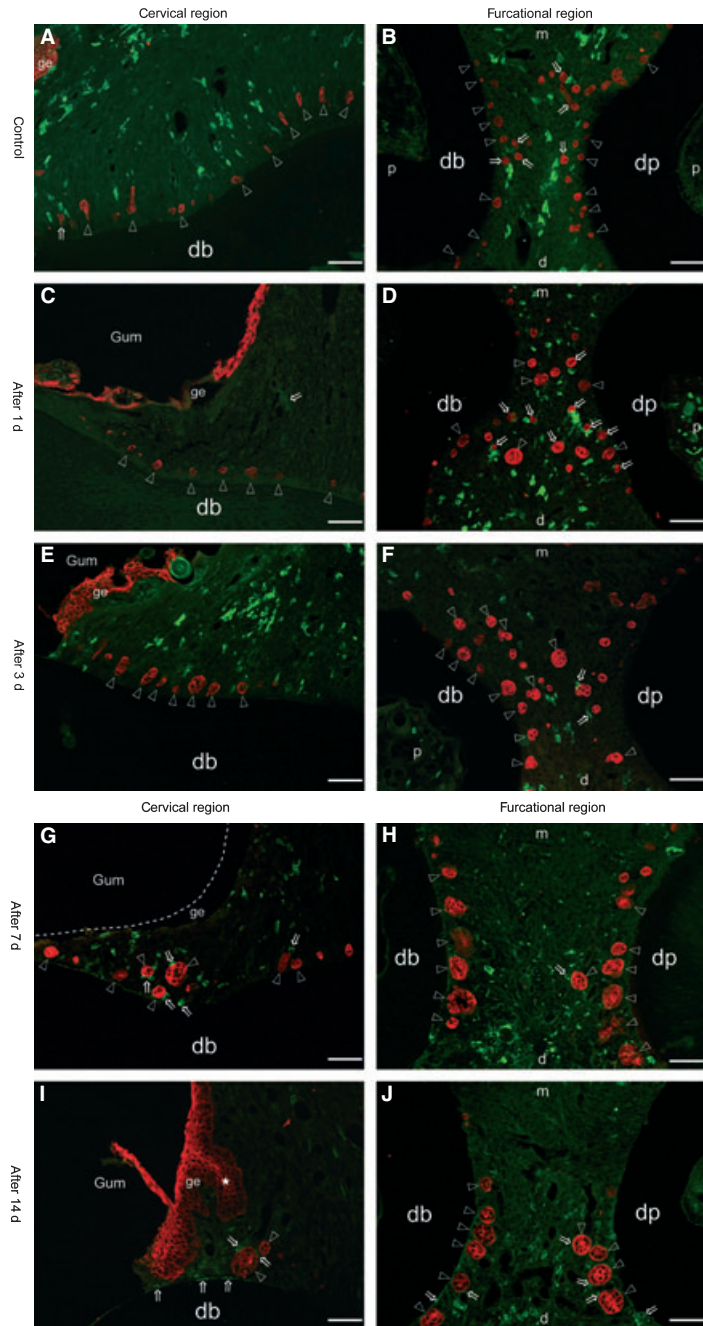


Fig. 5. Epithelial cell clusters (red) and OX6-immunopositive cells (green) in the cervical and furcational regions of the first molar periodontal ligament are shown. In all pictures, arrowheads indicate epithelial cell clusters and arrows show epithelial cell clusters contiguous with OX6-immunopositive cells. In the control group, epithelial cell clusters were present on the root surface and showed a spindle or oval shape in both regions. In the experimental group, large epithelial cell clusters appeared in the periodontal ligament near the gum insertion site with time, and the clusters were contiguous with or contacted each other. The OX6-immunopositive cells were contiguous with large cell clusters. Cell clusters became small and the between-cell cluster intervals widened as the distance from the gum insertion site increased. Dotted lines in (G) indicate gingival epithelium. The top and the bottom of the photos in the cervical region (A,C,E,G,I) have been flipped, and the left side indicates the gum insertion site (gum; C,E,G,I). Abbreviations: d, distal site (periodontal ligament near gum insertion site); db, disto-buccal root; dp, disto-palatal root; ge, gingival epithelium; m, mesial site (periodontal ligament distant from gum insertion site); p, pulp. Scale bars represent 50 μ m.

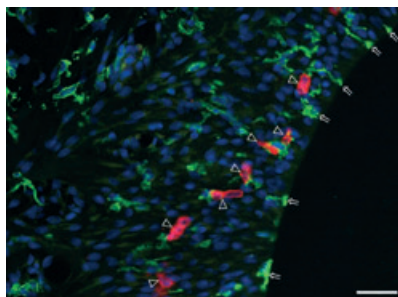


Fig. 6. Epithelial cell clusters (red) and OX6-immunopositive cells (green) in the first molar cervical region on day 3 are shown. The OX6-immunopositive cells extending cytoplasmic dendritic processes were abundantly distributed in the periodontal ligament and close to epithelial cell clusters (arrowheads) and the root surface (arrows) of the disto-palatal root. The bottom of the photograph is the periodontal ligament near the gum insertion site. The nuclei were stained with DAPI. Scale bar represents 50 μ m.

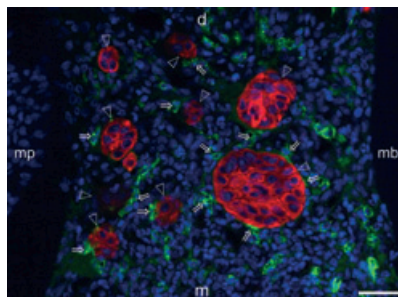


Fig. 7. Epithelial cell clusters (red) and OX6-immunopositive cells (green) in the second molar furcational region on day 7 are shown. Large cell clusters (arrowheads) were often noted in the periodontal ligament near the gum insertion site and the clusters were surrounded by OX6-immunopositive cells (arrows). The nuclei were stained with DAPI. Abbreviations: d, distal site (periodontal ligament distant from gum insertion site); mb, mesio-buccal root; mp, mesio-palatal root; m, mesial site (periodontal ligament near gum insertion site). Scale bar represents 50 μ m.

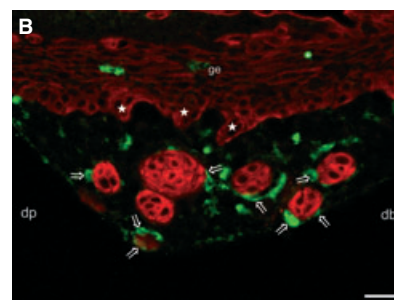
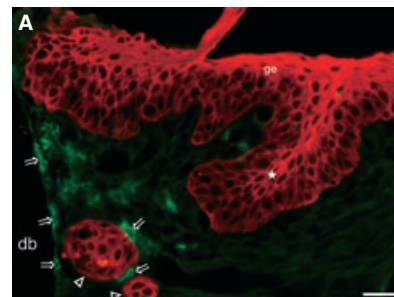


Fig. 8. Gingival epithelium, epithelial cell clusters (red) and OX6-immunopositive cells (green) in the first molar cervical (A); higher magnification of Fig. 5I) and furcational regions (B) on day 14 are shown. (A) Thickened gingival epithelium (ge) facing the inserted gum and cell clusters (arrowheads) were present in the cervical region, and a developed rete peg (star) reached proximal to the cell clusters. A small cell cluster was found close to the large cluster, and an OX6-immunopositive cell was also found in between the two clusters. The OX6-immunopositive cells (arrows) were in contact with cell clusters. The OX6-immunopositive cells were also in contact with the root surface. Slight unevenness was noted on the contacted surface. (B) The epithelium facing the inserted gum was thickened in the furcational region, as well as in the cervical region, and finger-like rete pegs (stars) were found proximal to cell clusters. Cell clusters were contiguous with each other and surrounded by OX6-immunopositive cells (arrows). Abbreviations: db, disto-buccal root; dp, disto-palatal root; ge, gingival epithelium. Scale bars represent 50 μ m.

often present near the root surface and arranged at regular intervals (Fig. 5F). The OX6-immunopositive reaction was localized in small spindle-shaped cells extending short cytoplasmic processes and occasionally surrounded CK-immunopositive cell clusters (Fig. 5F).

Periodontal ligament after 7 d

Cervical region— A CK-immunopositive reaction was noted in round or oval cell clusters near the root surface (Fig. 5G). Cell clusters distant from the root surface were often noted in connective tissue near the gingival epithelium pressed by the gum, and the cell clusters were contiguous with each other (Fig. 5G). An OX6-immunopositive reaction was noted in small cells extending short processes. The OX6-immunopositive cells were often present on the root surface and around CK-immunopositive cell clusters (Fig. 5G).

Furcational region— A CK-immunopositive reaction was noted in oval cell clusters near the root surface (Fig. 5H). On the root surface on the side near the gum insertion site, large cell clusters were often noted and they were contiguous with each other

(Fig. 5H). Cell clusters gradually became small and the interval between them increased as the distance from the gum insertion site grew. The size of cell clusters was markedly different between clusters near and distant from the gum insertion site. The OX6-immunopositive cells were mainly distributed in the periodontal ligament on the side near the gum insertion site and around CK-immunopositive cell clusters (Fig. 5H). In the second molar periodontal ligament near the gum insertion site, markedly large cell clusters and surrounding OX6-immunopositive cells were noted in the central region (Fig. 7).

Periodontal ligament after 14 d

Cervical region— A CK-immunopositive reaction was noted in oval cell clusters with various sizes near the root surface (Fig. 5I). Thick rete pegs extended into periodontal ligament from gingival epithelium, and their tips reached proximal to large cell clusters (Figs 5I and 8A). The OX6-immunopositive cells were widely distributed in the periodontal ligament and often contiguous with the root surface and CK-immunopositive cell clusters (Fig. 8A).

Furcational region— A CK-immunopositive reaction was noted in round or oval cell clusters near the root surface (Fig. 5J). On the root surface on the side near the gum insertion site, cell clusters with a size similar to that noted on day 7 were often present and these were contiguous with or closely contacted each other (Fig. 5J). With

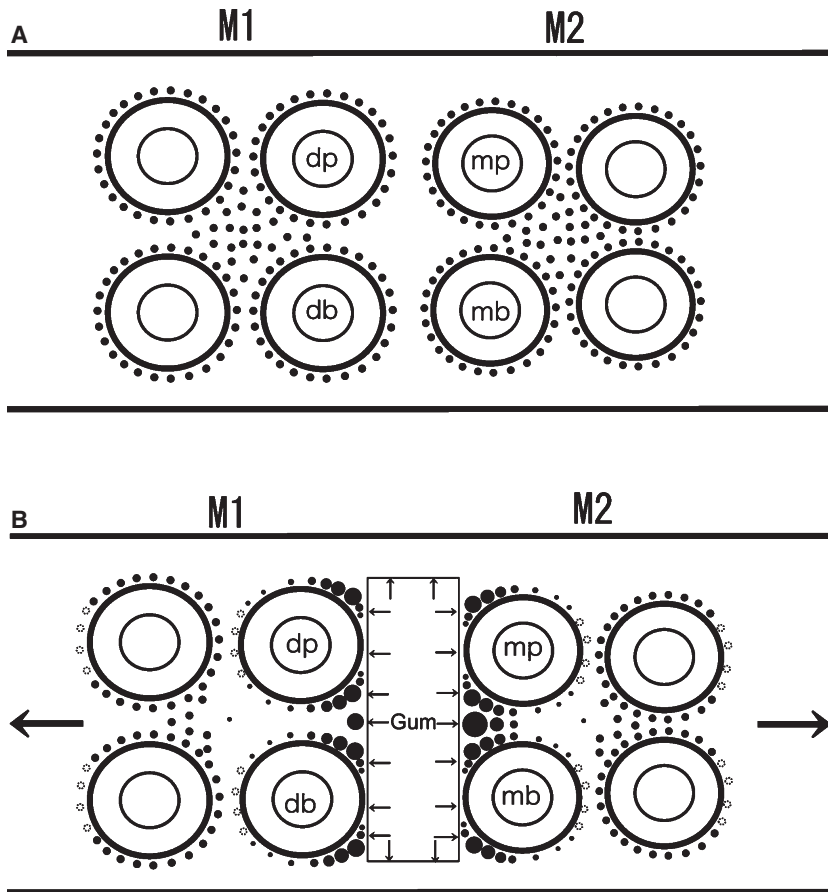


Fig. 9. (A) In the normal periodontal ligament, cell clusters are distributed around the furcation of the root of the tooth and each root. (B) After gum insertion, large cell clusters were often observed in the periodontal ligament near the insertion site, but small cell clusters were scattered in regions distant from the insertion site. Arrows in the rectangular portion represent directions of elastic force. The open star symbols represent compressed and disappeared cell clusters between root surface and alveolar bone. Abbreviations: db, disto-buccal root; dp, disto-palatal root; mb, mesio-buccal root; mp, mesio-palatal root.

increasing distance from the gum insertion site, cell clusters in the periodontal ligament became sparse. The cell cluster size was markedly different between those near and distant from the gum, and the difference increased compared with that on day 7. The OX6-immunopositive cells were abundant in the periodontal ligament near the gum insertion site and present on the root surface and around large CK-immunopositive cell clusters (Fig. 5J). On day 14, the gingival epithelium was markedly thickened, in a similar manner to that noted in the cervical region, and rete pegs were contiguous with oval cell clusters (Fig. 8B). The OX6-immunopositive cells often surrounded cell clusters.

The above findings are summarized schematically as cell cluster distributions before and after gum insertion (Fig. 9).

Discussion

The present study reports morphological evidence of reactions of periodontal ligament epithelial cell clusters and OX6-immunopositive cells to gum insertion between rat upper molars. Significant reactions of cell clusters and OX6-immunopositive cells were observed in the periodontal ligament near the insertion site. The CK-immunopositive cell rate increased significantly throughout the experimental period after 3 d, suggesting epithelial

cell proliferation in both the buccal and the furcational area. The results partly confirm our hypothesis.

The reaction of the cell clusters was divided into the following steps: arrangement at regular intervals, changes in the cell cluster morphology (round cell clusters increased while spindle-shaped cell clusters became rare), the intervals and arrangement were disturbed and cell clusters came close to each other, while large cell clusters appeared in the periodontal ligament near the insertion site. It has been reported that external stimulation, such as wound healing, mechanical stimulation in culture, and treatment with methyl nitrosourea stimulates the formation of large epithelial cell clusters (6,15,16). In a study which quantitatively analyzed the surface area of cell clusters for 6–72 h in similar conditions to those in the present study, the cell cluster surface area increased with time, and the clusters were bromo-deoxyuridine positive (7). In the present study, the cell cluster reaction was investigated for 14 d, and a marked difference was noted in the cell cluster size and rate between the control specimens and 3, 7 and 14 d. It is possible that the mechanical load on the periodontal ligament decreased due to a loss of gum elasticity after day 7, inflammation reduced, or the condition entered a chronic state. In contrast, in the region distant from the gum insertion site, i.e. mesial periodontal ligament from the region with large cell clusters, none of the above changes was noted. Considering these findings with the motility and clustering ability of periodontal ligament epithelial cells (17,18), the reactions can be interpreted as biological defense reactions of the periodontal ligament epithelial cells. It is necessary to verify the findings quantitatively in each region by long-term observation and the investigation of adhesion molecule expression, proliferative activity and cell death, such as apoptosis and necrosis, of cell clusters. Cell cluster reactions to loads applied employing a different method and movement in different directions are also of interest.

In rat periodontal ligament, an OX6-immunopositive reaction is detected on the cell membranes of dendritic cells, macrophages and B lymphocytes (19,20). OX6-immunopositive cells in the rat periodontal ligament are mostly dendritic cells and macrophages and contribute to the prevention of periodontal ligament infection, i.e. maintenance of the homeostasis of a healthy periodontal ligament. In reports focusing on the relationship between OX6-immunopositive cells and epithelial cell clusters, OX6-immunopositive cells sometimes surrounded cell clusters by extending dendritic cytoplasmic processes, and the two different cells interdigitated by each cytoplasmic process (10). In the present study, cell clusters and OX6-immunopositive cells were abundant near the gum insertion site, in the buccal/cervical area, and they were often contiguous. The OX6-immunopositive cell rate decreased in the furcation area at 1 and 3 d, most probably due to tissue disorganization. At 7 and 14 d, when periodontal ligament reparative processes activated (11), the cell rate normalized. Immunopositive cells and epithelial cell clusters may have interacted through the paracrine secretion of cytokines, such as interleukin-1, which are involved in the regulation of proliferative activity during inflammation (21–24).

It has been demonstrated that periodontal ligament epithelial cells express hard tissue-forming proteins, such as amelogenin, alkaline phosphatase and osteopontin, in response to interaction with fibroblasts, and their involvement in cementum formation has been suggested (25–27). In the rat periodontal ligament, OX6-immunopositive cells were also observed between epithelial cell clusters and fibroblasts, suggesting the involvement of OX6-immunopositive cells in the interaction of epithelial cells with fibroblasts (10). Attention should be paid to the relationship among these three cell types and expression of the above hard tissue-forming proteins.

Junctional epithelium and periodontal ligament epithelial cell clusters are contiguous with each other and assumed to be closely related embryo-

logically and functionally (28,29), but continuity between the epithelium and the clusters is mostly disrupted in normal periodontium. In contrast, apparent continuity between the epithelium and cell clusters in chronic periodontitis has been demonstrated (30,31). A high-level homology of the cell skeleton comprising the two tissues has been shown (4). Although Waldo's method is not only used in the orthodontic field (32,33), but also in studies on periodontal disease (34,35), no study on the relationship between the epithelium and periodontal ligament epithelial cell clusters has been reported. While no continuity was present between the gingival epithelial rete pegs and periodontal ligament epithelial cell clusters in the control group and in the early stage, stratified gingival epithelium and elongated rete pegs were found close to large cell clusters on day 14. The adjacent sections to those shown in Fig. 8 were carefully observed, but no apparent continuity was confirmed. However, epidermal growth factor receptor is strongly expressed on the cell cluster surface and in the inflammatory gingival epithelial basal layer (36), strongly suggesting that the proliferation and fusion of the rete pegs and periodontal ligament epithelial cell clusters can be observed by following time course of inflammatory changes, and this experimental model is useful to elucidate the involvement of periodontal ligament epithelial cell clusters in the mechanism establishing periodontitis.

In summary, elastic gum was inserted between the upper first and second molars in adult rats to move the teeth experimentally and induce periodontitis, and the reactions of periodontal ligament epithelial cell clusters and OX6-immunopositive cells were followed over time. As a result, the following observations were made: (i) large periodontal ligament epithelial cell clusters appeared and became contiguous, and OX6-immunopositive cells surrounded the clusters with time in the periodontal ligament near the gum insertion site; (ii) meanwhile, epithelial and OX6-immunopositive cells were scattered in the periodontal ligament distant from the gum insertion

site; and (iii) thickened epithelium and developed rete pegs were found close to large cell clusters on day 14. These findings imply proliferation and/or aggregation of periodontal ligament epithelial cell clusters in response to inflammation, and the regulation of activity by the interaction between OX6-immunopositive cells and cell clusters. In addition, this method was considered to be a useful model to elucidate the relationship between rete pegs and periodontal ligament epithelial cell clusters in inflammatory conditions.

Acknowledgements

This study was supported by a Grant-in-Aid for Scientific Research (no. 19791356) from the Ministry of Education, Science, Sports and Culture, Japan.

References

1. Valderhaug JP, Nylen MU. Function of epithelial rests as suggested by their ultrastructure. *J Periodontol Res* 1966; **1**:69–78.
2. Hamamoto Y, Nakajima T, Ozawa H. Ultrastructural and histochemical study on the morphogenesis of epithelial rests of Malassez. *Arch Histol Cytol* 1989; **52**:61–70.
3. Tadokoro O, Kawahara I, Vandevska-Radunovic V, Inoue K. Distribution of epithelial cells and their relationship to immunocompetent cells in rat molars: a confocal and transmission electron microscope study. *J Histochem Cytochem* 2009; **57**:315–325.
4. Peters BH, Peters JM, Kuhn C, Zöllner J, Franke WW. Maintenance of cell-type-specific cytoskeletal character in epithelial cells out of epithelial context: cytokeratins and other cytoskeletal proteins in the rests of Malassez of the periodontal ligament. *Differentiation* 1995; **59**:113–126.
5. Sculean A, Berakdar M, Pahl S *et al.* Patterns of cytokeratin expression in monkey and human periodontium following regenerative and conventional periodontal surgery. *J Periodontol Res* 2001; **36**:260–268.
6. Johansen JR. Incorporation of tritiated thymidine by the epithelial rests of Malassez after attempted extraction of rat molars. *Acta Odontol Scand* 1970; **28**:463–470.
7. Talic NF, Evans CA, Daniel JC, Zaki AE. Proliferation of epithelial rests of

- Malassez during experimental tooth movement. *Am J Orthod Dentofacial Orthop* 2003;**123**:527–533.
8. Gao Z, Mackenzie IC, Rittman BR, Korszum A-K, Williams DM, Crunchley AT. Immunohistochemical examination of immune cells in periapical granulomata and odontogenic cysts. *J Oral Pathol* 1988;**17**:84–90.
 9. Kan L, Okiji T, Kaneko T, H S. Localization and density of myeloid leucocytes in the periodontal ligament of normal rat molars. *Arch Oral Biol* 2001;**46**:509–520.
 10. Tadokoro O, Vandevska-Randunovic V, Inoue K. Epithelial cell rests of Malassez and OX6-immunopositive cells in the periodontal ligament of rat molars: a light and transmission electron microscope study. *Anat Rec* 2008;**291**:242–253.
 11. Vandevska-Radunovic V, Kvinnslund S, Jonsson R. Immunocompetent cells in rat periodontal ligament and their recruitment incident to experimental orthodontic tooth movement. *Eur J Oral Sci* 1997;**105**:36–44.
 12. Reitan K. Behavior of Malassez' epithelial rests during orthodontic tooth movement. *Acta Odontol Scand* 1961;**19**:443–468.
 13. Gilhuus-Moe O, Kvam E. Behaviour of the epithelial remnants of Malassez following experimental movement of rat molars. *Acta Odontol Scand* 1972;**30**:139–149.
 14. Waldo CM, Rothblatt JM. Histologic response to tooth movement in the laboratory rat: procedure and preliminary observations. *J Dent Res* 1954;**33**:481–486.
 15. Brunette DM. Mechanical stretching increases the number of epithelial cells synthesizing DNA in culture. *J Cell Sci* 1984;**69**:35–45.
 16. Hamamoto Y, Hamamoto N, Nakajima T, Ozawa H. Morphological changes of epithelial rests of Malassez in rat molars induced by local administration of N-methylnitrosourea. *Arch Oral Biol* 1998;**43**:899–906.
 17. Yamasaki A, Pinero GJ. An ultrastructural study of human epithelial rests of Malassez maintained in a differentiated state in vitro. *Arch Oral Biol* 1989;**34**:443–451.
 18. Birek P, Wang HM, Brunette DM, Melcher AH. Epithelial rests of Malassez in vitro. Phagocytosis of collagen and the possible role of their lysosomal enzymes in collagen degradation. *Lab Invest* 1980;**43**:61–72.
 19. McMaster WR, Williams AF. Identification of Ia glycoproteins in rat thymus and purification from rat spleen. *J Immunol* 1979;**9**:426–433.
 20. McMenamin PG, Holthouse I, Holt PG. Class II major histocompatibility complex (Ia) antigen-bearing dendritic cells within the iris and ciliary body of the rat eye: distribution, phenotype and relation to retinal microglia. *Immunology* 1992;**77**:385–393.
 21. Liu F, Abiko Y, Nishimura M, Kusano K, Shi S, Kaku T. Expression of inflammatory cytokines and beta-defensin 1 mRNAs in porcine epithelial rests of Malassez in vitro. *Med Electron Microsc* 2001;**34**:174–8.
 22. Lossdörfer S, Götz W, Jäger A. Localization of IL-1alpha, IL-1 RI, TNF, TNF-RI and TNF-RII during physiological drift of rat molar teeth – an immunohistochemical and in situ hybridization study. *Cytokine* 2002;**20**:7–16.
 23. Miyauchi M, Sato S, Kitagawa S *et al*. Cytokine expression in rat molar gingival periodontal tissues after topical application of lipopolysaccharide. *Histochem Cell Biol* 2001;**116**:57–62.
 24. Ohshima M, Yamaguchi Y, Micke P, Abiko Y, Otsuka K. In vitro characterization of the cytokine profile of the epithelial cell rests of Malassez. *J Periodontol* 2008;**79**:912–919.
 25. Hasegawa N, Kawaguchi H, Ogawa T, Uchida T, Kurihara H. Immunohistochemical characteristics of epithelial cell rests of Malassez during cementum repair. *J Periodontol Res* 2003;**38**:51–56.
 26. Rincon JC, Xiao Y, Young WG, Bartold PM. Production of osteopontin by cultured porcine epithelial cell rests of Malassez. *J Periodontol Res* 2005;**40**:417–426.
 27. Shimonishi M, Hatakeyama J, Sasano Y *et al*. In vitro differentiation of epithelial cells cultured from human periodontal ligament. *J Periodontol Res* 2007;**42**:456–65.
 28. Spouge JD. A new look at the rests of Malassez. A review of their embryological origin, anatomy, and possible role in periodontal health and disease. *J Periodontol* 1980;**51**:437–444.
 29. Woodnutt DA, Byers MR. Morphological variation in the tyrosine receptor kinase A-immunoreactive periodontal ligament epithelium of developing and mature rats. *Arch Oral Biol* 2001;**46**:163–171.
 30. Spouge JD. The rests of Malassez and chronic marginal periodontitis. *J Clin Periodontol* 1984;**11**:340–347.
 31. Spouge JD. A study of epithelial odontogenic residues in the pig. *J Periodontol* 1986;**57**:164–171.
 32. Kobayashi H, Ochi K, Saito I, Hanada K, Maeda T. Alterations in ultrastructural localization of growth-associated protein-43 (GAP-43) in periodontal Ruffini endings of rat molars during experimental tooth movement. *J Dent Res* 1998;**77**:503–517.
 33. Yokoya K, Sasaki T, Shibasaki Y. Distributional changes of osteoclasts and pre-osteoclastic cells in periodontal tissues during experimental tooth movement as revealed by quantitative immunohistochemistry of H(+)-ATPase. *J Dent Res* 1997;**76**:580–587.
 34. Abiko Y, Shimono M. An ultrastructural study of the pocket epithelium in rats. *Bull Tokyo Dent Coll* 1991;**32**:27–34.
 35. Uno T, Hashimoto S, Shimono M. A study of the proliferative activity of the long junctional epithelium using argyrophilic nucleolar organizer region (AgNORs) staining. *J Periodontol Res* 1998;**33**:298–309.
 36. Nordlund L, Hormia M, Saxén L, Thesleff I. Immunohistochemical localization of epidermal growth factor receptors in human gingival epithelia. *J Periodontol Res* 1991;**26**:333–338.

This document is a scanned copy of a printed document. No warranty is given about the accuracy of the copy. Users should refer to the original published version of the material.